AMERICAN ACADEMY™ OF OPHTHALMOLOGY

Posterior Vitreous Detachment and the Posterior Hyaloid Membrane

Gregory S. Fincham, MD(Res), FRCOphth,[1] Sean James, MSc,[2] Carl Spickett, PhD,[3] Michael Hollingshead, PhD,[3] Christopher Thrasivoulou, PhD,[4] Arabella V. Poulson, FRCOphth,[1] Annie McNinch, SRN,[1,3] Allan Richards, PhD,[3,5] David Snead, FRCPath,[2] Gloria A. Limb, PhD,[6] Martin P. Snead, MD, FRCOphth[1,3]

Purpose: Despite posterior vitreous detachment being a common ocular event affecting most individuals in an aging population, there is little consensus regarding its precise anatomic definition. We investigated the morphologic appearance and molecular composition of the posterior hyaloid membrane to determine whether the structure clinically observed enveloping the posterior vitreous surface after posterior vitreous detachment is a true basement membrane and to postulate its origin. Understanding the relationship between the vitreous (in both its attached and detached state) and the internal limiting membrane of the retina is essential to understanding the cause of rhegmatogenous retinal detachment and vitreoretinal interface disorders, as well as potential future prophylactic and treatment strategies.

Design: Clinicohistologic correlation study.

Participants: Thirty-six human donor globes.

Methods: Vitreous bodies identified to have posterior vitreous detachment were examined with phase-contrast microscopy and confocal microscopy after immunohistochemically staining for collagen IV basement membrane markers, in addition to extracellular proteins that characterize the vitreoretinal junction (fibronectin, laminin) and vitreous gel (opticin) markers. The posterior retina similarly was stained to evaluate the internal limiting membrane. Findings were correlated to the clinical appearance of the posterior hyaloid membrane observed during slit-lamp biomicroscopy after posterior vitreous detachment and compared with previously published studies.

Main Outcome Measures: Morphologic appearance and molecular composition of the posterior hyaloid membrane.

Results: Phase-contrast microscopy consistently identified a creased and distinct glassy membranous sheet enveloping the posterior vitreous surface, correlating closely with the posterior hyaloid membrane observed during slit-lamp biomicroscopy in patients with posterior vitreous detachment. Immunofluorescent confocal micrographs demonstrated the enveloping membranous structure identified on phase-contrast microscopy to show positive stain results for type IV collagen. Immunofluorescence of the residual intact internal limiting membrane on the retinal surface also showed positive stain results for type IV collagen.

Conclusions: The results of this study provide immunohistochemical evidence that the posterior hyaloid membrane is a true basement membrane enveloping the posterior hyaloid surface. Because this membranous structure is observed only after posterior vitreous detachment, the results of this study indicate that it forms part of the internal limiting membrane when the vitreous is in its attached state. *Ophthalmology 2018;125:227-236*

Supplemental material available at www.aaojournal.org.

The vitreous humor is the largest anatomic structure in the human eye; it is a specialized transparent connective tissue that fills the posterior segment of the eye, occupying more than three quarters of the total ocular volume. In common with all connective tissues, which are separated from their adjacent epithelium, mesothelium, or endothelium by true basement membranes composed of type IV collagen,[1] the vitreous is separated from its adjacent neuroepithelium (retina) by the internal limiting membrane composed of type IV collagen.[2]

Uniquely in humans, the vitreous undergoes a progressive morphologic remodelling with an increase in fluid-filled lacunae (synchysis)[3] and an increase in collagenous condensations (syneresis)[4] as part of the aging process. In youth, collagen fibrils of the posterior vitreous cortex are firmly adherent to the internal limiting membrane of the retina by proteoglycans, including laminin and fibronectin.[5–8] Both vitreous syneresis and posterior vitreous detachment are thought to be influenced by age and refractive error, but are separate pathologic entities and frequently occur independently of the other.[3,9,10] Posterior vitreous detachment may be an asymptomatic finding in many patients; however, in those patients who are symptomatic, separation of the vitreous from the retina is

http://dx.doi.org/10.1016/j.ophtha.2017.08.001
ISSN 0161-6420/17

associated with an acute onset of flashes and floaters. Flashes refer to the pathognomonic features of temporal photopsia, described as a momentary arc of white or golden light in the lateral field of vision, whereas floaters refer to the subjective perception of the shadows cast onto the retina by vitreal opacities.[11,12] Despite being a common ocular event affecting most individuals in an aging population,[13–15] there is still recognized difficulty in making an accurate diagnosis in all cases and little agreement regarding the precise anatomic definition of posterior vitreous detachment.

Imaging-based diagnosis of posterior vitreous detachment traditionally has relied on dynamic B-scan ultrasonography; with an experienced operator, it reliably correlates to clinical biomicroscopy and intraoperative evidence of posterior vitreous detachment.[16] More recently, OCT has been introduced in an attempt to objectify and standardize the diagnosis of posterior vitreous detachment. Although initial correlations to clinical and intraoperative posterior vitreous detachment have been limited,[16,17] developments in increased-resolution spectral-domain OCT, wide-field scanning patterns, dynamic examination protocols, and combination imaging with scanning laser ophthalmoscopy promise to improve the potential of this imaging method to diagnose posterior vitreous detachment reliably in the future.[18,19]

The generally accepted consensus regarding the definition and diagnosis of posterior vitreous detachment is that there is a separation of the condensed outer layers of type II collagen fibrils of the vitreous, known as the posterior vitreous cortex, from the internal limiting membrane of the retina.[20–24] The term *posterior hyaloid face* is used commonly to describe the outermost cortical layer of the vitreous. Clinical diagnosis of a suspected posterior vitreous detachment is based on the clinical history of new-onset flashes and floaters, with or without the identification of epipapillary glial tissue torn form the optic nerve head (Weiss ring) noted in the posterior vitreous cortex on slit-lamp biomicroscopy.[25–27]

An alternative, more stringent clinical interpretation defines posterior vitreous detachment as the separation of the vitreous and its enveloping posterior hyaloid membrane from the surface of the retina.[12,28,29] Proponents of this concept advocate the term *posterior hyaloid membrane* to describe the membranous structure visualized on slit-lamp biomicroscopy encasing the detached vitreous. Clinical diagnosis of a suspected posterior vitreous detachment is based on clinical history, in addition to the identification of a continuous, discrete, highly creased, and refractile membranous sheet observed by slit-lamp dynamic vitreous biomicroscopy with a wide illumination observation angle (Fig 1; Video 1, available at www.aaojournal.org). It follows that notwithstanding any associated syneresis within the gel itself, this structure must form part of the vitreoretinal interface and internal limiting membrane immediately before vitreous detachment.

Previous studies examining patients with and without posterior vitreous detachment antemortem and correlating the findings with the postmortem histologic investigation of the vitreous in the same patients demonstrated that cadaveric posterior vitreous detachment is consistent with, and a true representation of, antemortem posterior vitreous detachment.[14,30] This study compared the histopathologic and immunohistochemical profiles of the posterior hyaloid membrane in donated human globes with posterior vitreous detachment.

Methods

Study Design

The posterior surface of the vitreous body in donated human globes identified to have posterior vitreous detachment was interrogated with phase-contrast microscopy and subsequently histochemically stained for basement membrane (collagen IV), vitreoretinal junction (fibronectin, laminin), and vitreous gel (opticin) markers to facilitate immunofluorescent confocal microscopy analysis. The posterior retina similarly was stained with collagen IV immunofluorescence to evaluate the status of the remaining internal limiting membrane. The resultant micrographs were compared with the clinical appearance of the posterior hyaloid membrane observed during slit-lamp biomicroscopy examination of patients with posterior vitreous detachment.

Materials

Under a material transfer agreement, the Corneal Transplant Service Eye Bank, University of Bristol, supplied human globe tissue after harvesting an anterior segment 18-mm corneoscleral button for corneal transplantation surgery. The globe tissue, which comprised all ocular structures internal to and including the scleral coat posteriorly and the iris anteriorly, was fixed in 4% paraformaldehyde at 4°C and transported by cold chain courier. Upon receipt, the globe tissue was rinsed repeatedly in cold phosphate-buffered saline, cryoprotected in a 30% sucrose and phosphate-buffered saline solution, frozen in acetone chilled in liquid nitrogen, and stored at −80°C before being thawed on ice for dissection at room temperature.

Dissection Protocol

To evaluate posterior vitreous detachment status, a modification to the suspended-in-air examination, originally described by Foos,[31] was used. A circumferential full-thickness scleral coat incision into the suprachoroidal space was placed around the optic nerve stalk posteriorly. Anteriorly, the iris was removed circumferentially at its root. Radial full-thickness scleral incisions (connecting the anterior scleral edge to the posterior peripapillary incision) facilitated removal of the scleral coat from the remaining eviscerated vitreous body, covered by retina and choroid, and attached posteriorly to the optic nerve stalk and surrounding rim of scleral tissue.

The modification of Foos' air suspension technique assessed the posterior vitreous detachment status before and after removal of the choroid. Upon removal of the choroid, the retina of specimens with a posterior vitreous detachment would tear at their firm anterior attachment to the vitreous base under the weight of the vitreous body, leaving the denuded posterior surface of the vitreous body exposed. In distinct contrast, those globes without posterior vitreous detachment were found to have retina adherent to the entire posterior vitreous surface that was possible to remove only with piecemeal dissection.

Posterior-to-anterior 18-mm trephination through the vitreous body in specimens with posterior vitreous detachment allowed removal of the anterior annulus of retinal tissue attached to the vitreous base and peripheral anterior vitreous gel. This yielded a

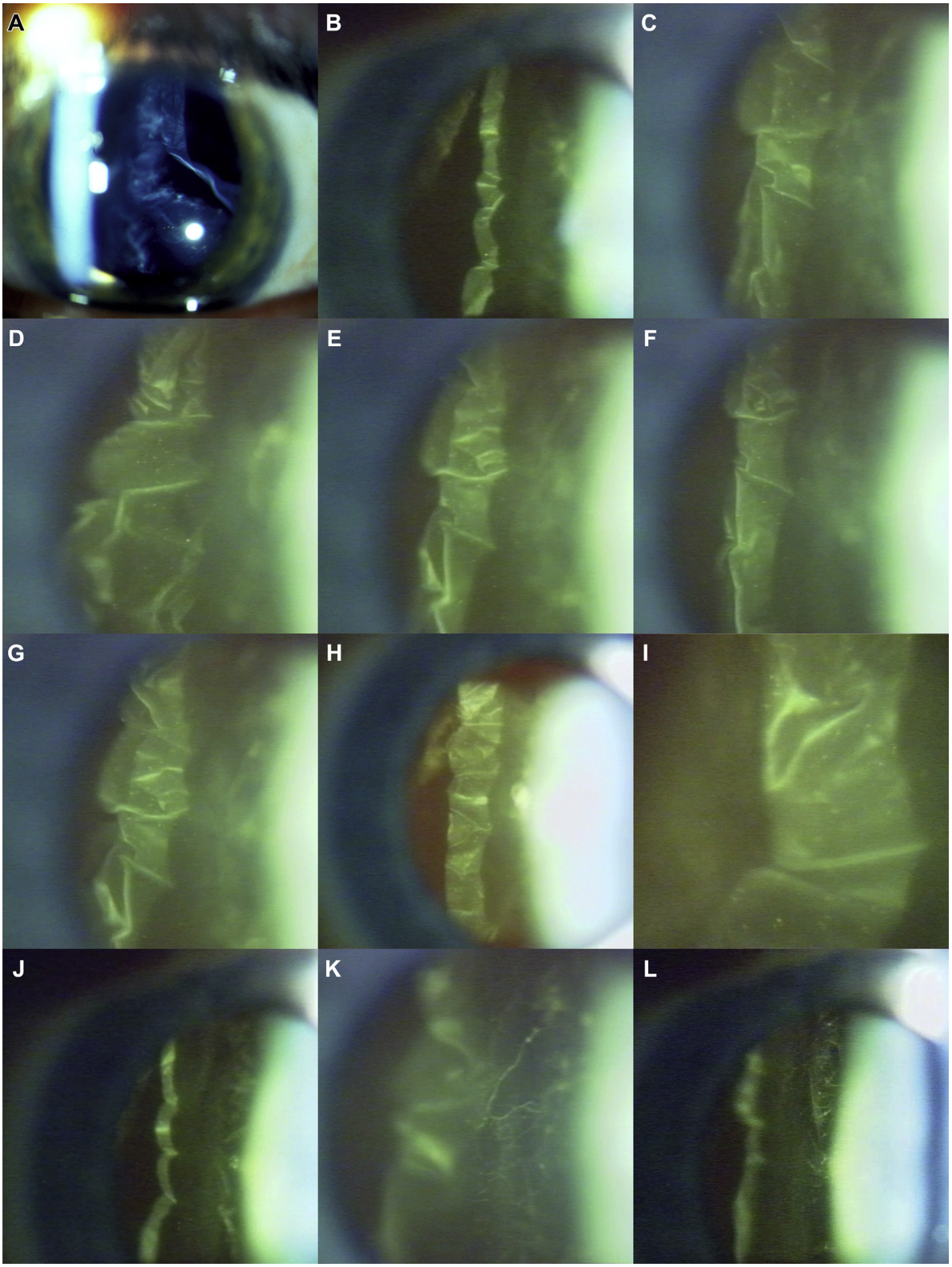

Figure 1. Dynamic off-axis illumination slit-lamp biomicroscopy images demonstrating the clinical appearance of the posterior hyaloid membrane in a patient with posterior vitreous detachment. Note the classic creased and crinkled topographic appearance (**A**–**I**), in addition to the vitreous fibrils anterior to the membrane in (**J**–**L**). See Video 1 (available at www.aaojournal.org).

core of clear vitreous gel with its associated posterior hyaloid membrane lining the posterior vitreous surface, which then was examined by phase-contrast microscopy and immunohistochemical staining for collagen IV. Posterior pole retinal tissue from specimens with identified posterior vitreous detachment was collected for immunohistochemical staining of the internal limiting membrane.

Phase-Contrast Microscopy

The posterior surface of the trephined gel core was examined using a Zeiss Primo Vert phase-contrast light microscope (Zeiss, Germany) to identify the posterior hyaloid membrane.

Immunohistochemistry Analysis

Examined tissue was blocked and permeabilized overnight at 4°C in phosphate-buffered saline with 1:20 donkey serum, 0.5% bovine serum albumin, and 0.1% TritonTM.1 X-100; this also was used for all subsequent washes and to dilute antibodies. Primary and secondary antibodies were incubated sequentially over consecutive nights at 4°C; 3 blocking solution washes were performed before and after secondary antibody incubation. Tissues then were flat mounted in a prepared water-based mounting medium (6 g glycerol, 2.4 g Moviol 4-88 (Hoechst, Germany), 6 ml nuclease-free water, and 12 ml tris(hydroxymethyl)aminomethane buffer) and covered with Leica Surgipath coverslips for confocal microscopy (Leica, Germany). Primary and secondary antibody concentrations were based on the recommended dilutions reported in similar immunofluorescent applications and optimized further using serial dilutions. Details of primary and secondary antibody sources and dilutions used are shown in Table 1.

Confocal Microscopy

Digital confocal micrograph images were acquired on a Zeiss Observer Z1 inverted LSM 700 Confocal Laser Scanning Microscope (Zeiss, Germany). Separation of fluorescence signals by sequential laser frequency excitation at 400, 440, 470, and 535 nm prevented multichannel crosstalk. Generated.lsm data files were processed with Carl Zeiss ZEN 2012 SP1 (black edition) software. Scanning protocols included phase and confocal low-magnification (EC Plan-Neofluar 10×0.30 Ph1 M27 Objective [Zeiss, Germany]) composite tile scans to ascertain global topography of posterior hyaloid membrane specimens, in addition to phase and confocal high-magnification (EC Plan-Apochromat 63×1.40 Oil Ph3 M27 Objective) z-stack imaging.

Control Tissue

Positive and negative control experiments were conducted for all tissues. Basement membrane control tissue was obtained from human kidney (under a material transfer agreement with the Arden Tissue Bank, University Hospital Coventry) and intraocular crystalline lens capsule (isolated from donated specimen without posterior vitreous detachment). Vitreous gel, vitreoretinal junction, and retinal control tissue were obtained similarly from randomly selected human globe tissue without posterior vitreous detachment.

Ethical Approval

This project was conducted after National Research Ethics Service approval (identifier 05/Q2802/77), and all investigations were conducted in accordance with the tenets of the Declaration of Helsinki with regard to research on human tissue.

Results

Globe Tissue

Fifty-eight donated globes (average age, 67.4 years; range, 41–79 years) were dissected. Thirty-six globes (62.1%; average age, 70.1 years; range, 41–96 years) were identified to have sustained a posterior vitreous detachment and were selected for phase-contrast microscopy and immunofluorescence study. Twenty-two globes (37.9%; average age, 63.1 years; range, 49–79 years) were identified to have an attached vitreous and were selected randomly for control studies. The age of donor globes and incidence of posterior vitreous detachment in the current study are similar to those reported in previous studies.[3,12,14,30]

Phase-Contrast Microscopy

Isolated posterior hyaloid membranes consistently were identified as distinct, creased, and crinkled glassy sheets on phase-contrast microscopy (Fig 2A). Residual attached vitreous gel demonstrated a rucked and undulating appearance (Fig 2B and C), but was readily distinguishable from the adjacent posterior hyaloid membrane, which was phase dense with definitive, sharply cut edges (Fig 2D). Physically manipulating samples during visualization under direct phase-contrast microscopy further demonstrated differences between the posterior hyaloid membrane and the cortical vitreous gel. The membrane component was relatively inflexible and reluctant to unfold, remaining in a crumpled orientation, reflecting and reminiscent

Table 1. Primary and Secondary Antibodies

Antibody	Manufacturer	Catalog No.	Species	Dilution
Primary antibodies				
Anticollagen IV*	Abcam	ab6586	Rabbit polyclonal	1:100
Antifibronectin†	Abcam	ab26245	Mouse monoclonal (A17)	1:100
Antilaminin†	Abcam	ab11575	Rabbit polyclonal	1:200
Antiopticin‡	Abcam	ab170886	Rabbit monoclonal (EPR11980[B])	1:250
Secondary antibodies				
Alexa Fluor 488	Life Technologies	A21202	Donkey antimouse	1:500
Alexa Fluor 568	Life Technologies	A10042	Donkey antirabbit	1:500

*Basement membrane marker.
†Vitreoretinal junction marker.
‡Vitreous gel marker.

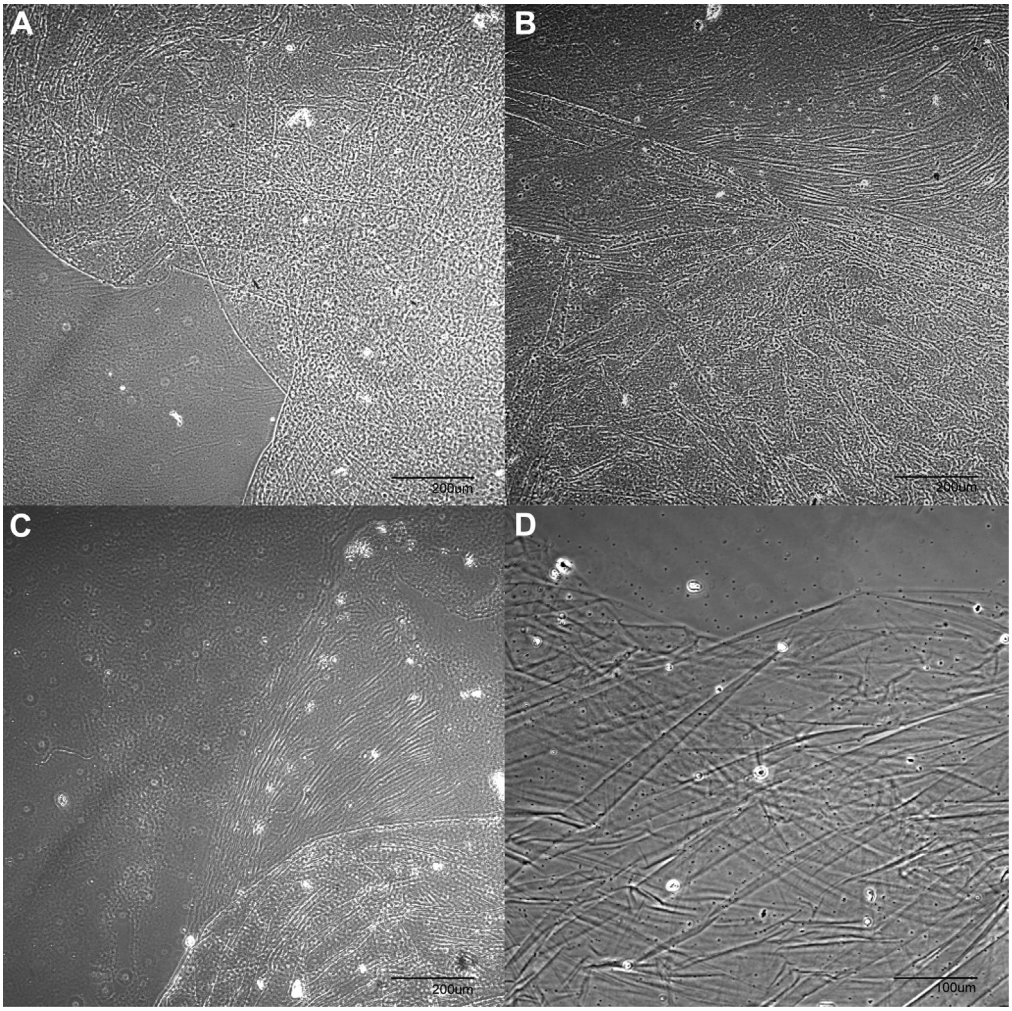

Figure 2. Phase-contrast micrographic series demonstrating (**A**) glassy, phase-dense appearance of the posterior hyaloid membrane (original magnification, ×5), (**B**) rippled vitreous gel appearance (*upper right corner*) adjacent to the posterior hyaloid membrane (lower half of image; original magnification, ×5), (**C**) distinct boundary between vitreous gel (*upper right corner*) and posterior hyaloid membrane (*lower right corner*; original magnification, ×5), and (**D**) high-power view illustrating a definitive cut edge of the posterior hyaloid membrane (original magnification, ×10).

of its characteristics observed during pars plana vitrectomy surgery. In contrast, the body of the vitreous gel had a pliable and elastic nature, returning to its original orientation after being handled.

Basement Membrane Immunohistochemistry Analysis

Posterior hyaloid membranes, isolated from globes that had undergone posterior vitreous detachment, consistently demonstrated positive immunofluorescence results with collagen IV antibodies, indicating they were true basement membranes. Confocal immunofluorescent images characterized membranous sheets with definitive, sharply cut edges (Fig 3A and B). Surface topography micrographs revealed these membranes to have a highly creased and crinkled appearance (Fig 3C), correlating with the membranous structure identified on phase-contrast microscopy. Z-stack cross section confocal analysis (Fig 3D) and 3-dimensional image reconstructions demonstrated a smooth configuration to the vitreal aspect (Fig 3E) and an irregular coarse configuration to the retinal aspect (Fig 3F) of the posterior hyaloid membrane.

Internal Limiting Membrane Immunohistochemistry

The posterior pole retina consistently demonstrated positive immunofluorescence with collagen IV antibodies, indicating an intact internal limiting membrane in globes that had undergone posterior vitreous detachment (Fig 4A and B). Immunofluorescent images of the retinal surface demonstrated a complete and continuous internal limiting membrane that was associated integrally with the anticipated vascular branching pattern of superficial retinal blood vessels, delineated by their endothelial basement membranes (Fig 4C and D).

Vitreoretinal Junction and Vitreous Gel Immunohistochemistry Analysis

Confocal microscopy of specimens stained with fibronectin and laminin antibody markers demonstrated these vitreoretinal junction

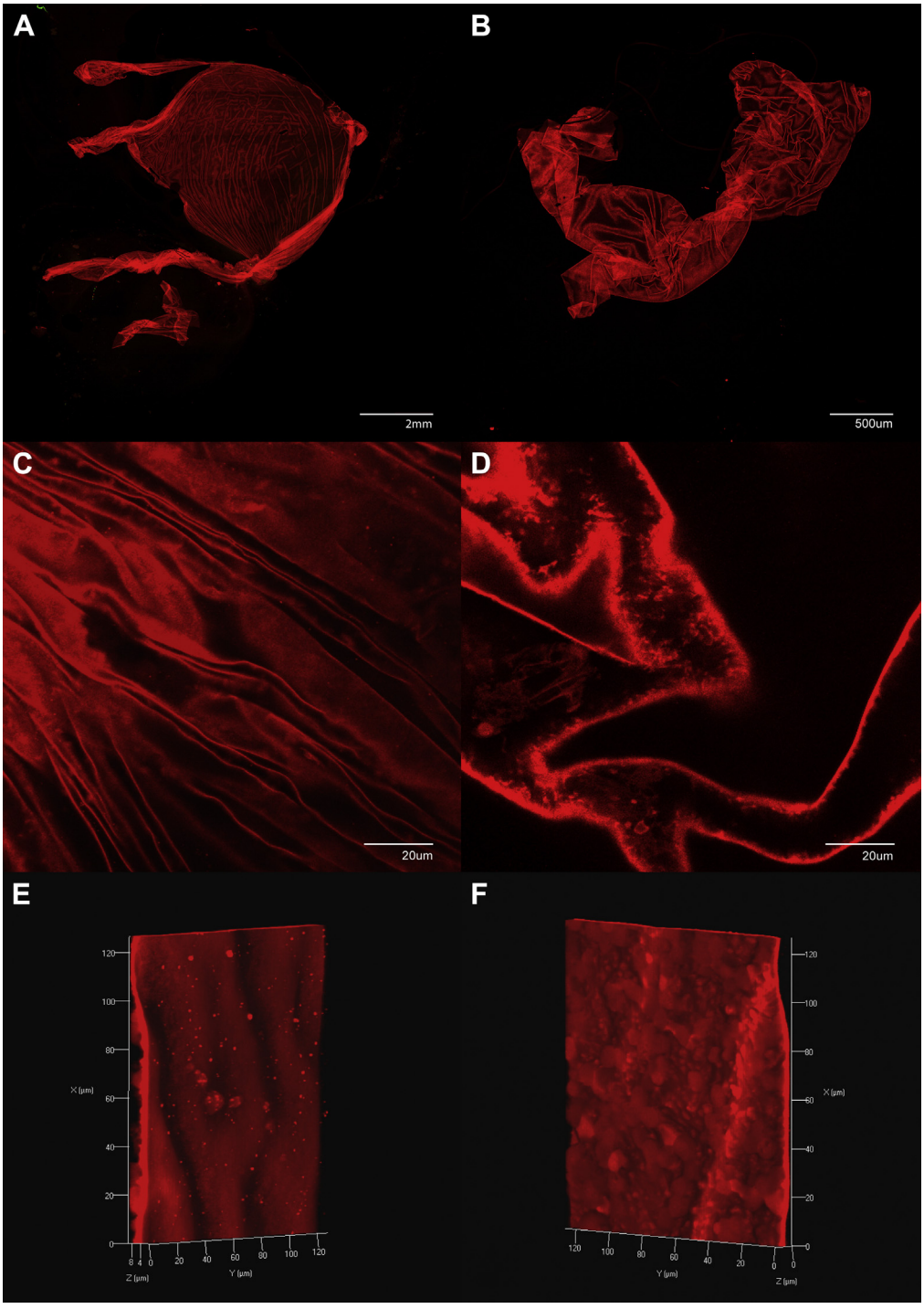

Figure 3. Posterior hyaloid membrane confocal micrography series stained with antibodies to collagen IV (Alexa Fluor 568), demonstrating (**A**) 10×10 tile scan (original magnification, ×5), (**B**) 3×3 tile scan (original magnification, ×5), (**C**) surface topography (original magnification, ×63), (**D**) z-stack cross section through the membrane fold (original magnification, ×63), and (**E**, **F**) 3-dimensional image reconstructions of the z-stack illustrating the smooth vitreal aspect and coarse retinal aspect of the posterior hyaloid membrane, respectively.

proteins to be distributed densely on the vitreal aspect of the detached posterior hyaloid membrane, as anticipated. Furthermore, the vitreous gel consistently demonstrated positive immunofluorescence with opticin antibodies. Staining delineated individual vitreous gel fibrils, with a distinct condensation of vitreal fibers observed at the gel—membrane interface.

Comparison of Findings with Clinically Observed Posterior Hyaloid Membranes

Distinct, highly creased and crinkled posterior hyaloid membrane phase-contrast (Fig 2) and immunofluorescent (Fig 3) micrographs consistently were similar in appearance to the posterior hyaloid

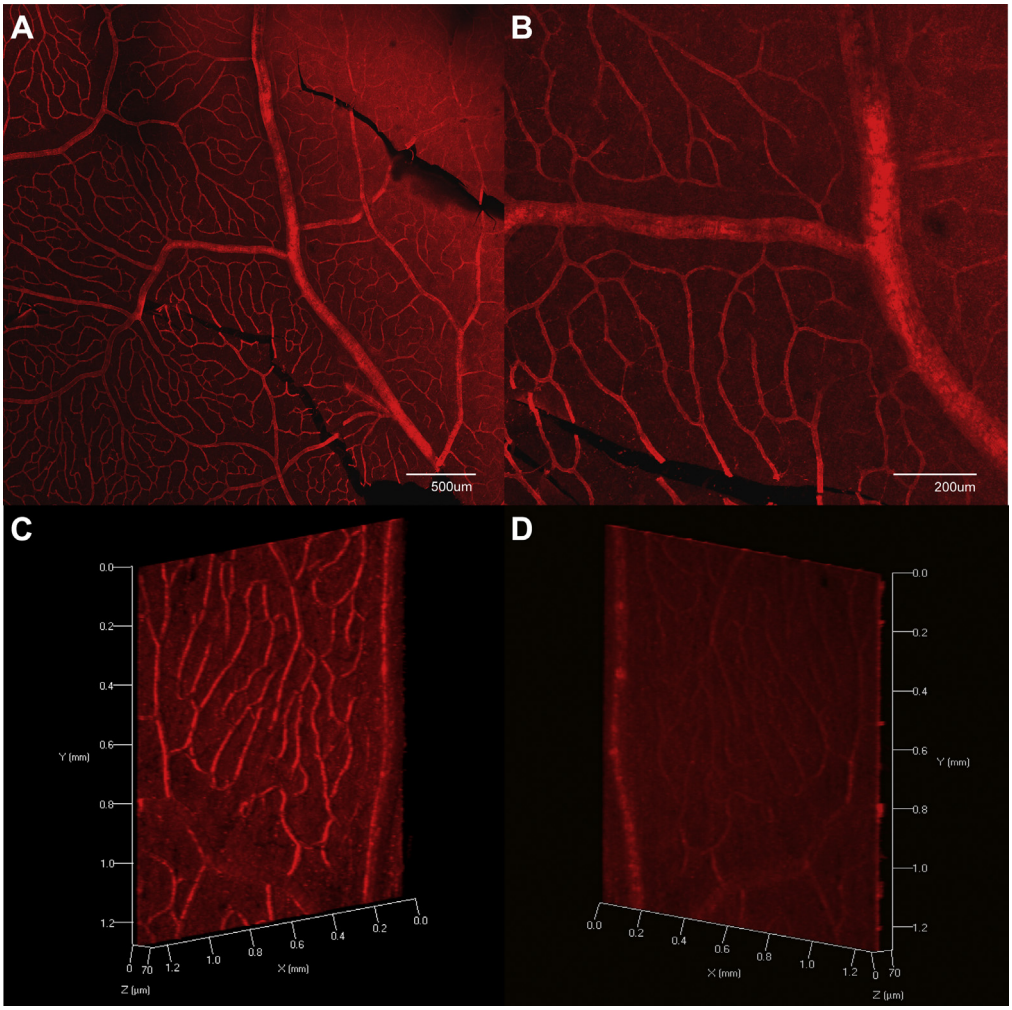

Figure 4. Internal limiting membrane confocal micrography series stained with antibodies to collagen IV (Alexa Fluor 568), demonstrating (**A**) 3×3 tile scan of the retinal posterior pole flat mount after posterior vitreous detachment (note greater internal limiting membrane immunofluorescence in the *upper right corner* compared with the *bottom left*, resulting from retinal undulation altering the focal plane; original magnification, ×5); (**B**) magnified view of artifactual retinal break in (**A**), demonstrating internal limiting membrane edge (original magnification, ×12.5); and (**C**, **D**) 3-dimensional reconstructions of the *z*-stack illustrating the relationship of the internal limiting membrane to the retinal microvascular network (retinal and vitreal aspects, respectively).

membranes observed clinically in patients with posterior vitreous detachment (Fig 1). Furthermore, manipulation of the membranes under phase-contrast microscopy produced movement patterns reminiscent of those witnessed with clinical off-axis illumination slit-lamp microscopy (Video 1, available at www.aaojournal.org).

Discussion

In addition to its anatomic location between the connective tissue of the vitreous body and the neuroepithelial retina, molecular interrogation of the internal limiting membrane has demonstrated it to be a true basement membrane composed of collagen IV,[2] laminin, fibronectin,[32] and carbohydrate residues.[33] The ultrastructure of the internal limiting membrane has been well characterized by electron microscopy. The original descriptions by Fine[34] and Fine and Tousimis[35] have been confirmed and reiterated in several subsequent studies[36–40] and have been expanded further by Foos.[41] Foos described variations of the internal limiting membrane in 3 distinct topographic zones within the eye; in the basal zone, the internal limiting membrane was uniformly thin, but it was reported to be progressively and irregularly thickened in the equatorial and posterior zones, in addition to showing loss of the anteriorly observed Müller vitreal surface attachment plaques in the posterior zone. Transmission electron micrographs demonstrated an enormous 37-fold increase in thickness of the posterior zone of the internal limiting membrane compared with the basal zone, with a characteristically smooth vitreal aspect and irregular retinal aspect following the contour of underlying Müller glia.

Seeking to investigate whether the internal limiting membrane thickened with age in a fashion consistent with other ocular basement membranes,[42,43] Heegaard[44] reported a series of adult eyes from the third to tenth decades of life and compared them with fetal eyes. The internal limiting

membrane of fetal eyes was found to be uniformly thin in all regions and followed the surface contour of Müller glia compared with the internal limiting membrane of adult eyes that reiterated similar topographically variant findings of progressive thickening and irregularity posteriorly (with a characteristic smooth inner vitreal surface and undulating outer cellular surface), as described by Foos.[41] Although the internal limiting membrane was found to be markedly thicker in adult eyes than in fetal eyes at 24 weeks' gestation, there was no reported statistical correlation of increasing thickness with increasing age; the author attributed the lack of trend to small study numbers (1 pair of eyes from 2 adults from each of the third through to the tenth decades, except for the sixth decade, where only 1 pair of eyes was obtained), in addition to technical issues of averaging median thickness values of a structure with complex external folds and using different examination techniques.

Reappraising Heegaard's original data, it is apparent that the maximum thickness of the internal limiting membrane at the posterior pole seemed to peak at between 30 and 50 years of age (median thickness, 3230 nm) in specimens examined by transmission electron microscopy and between 60 and 80 years of age (median thickness, 1336 nm) for specimens examined by scanning electron microscopy. A conceivable explanation may be that the thickness of the internal limiting membrane peaked between 40 to 70 years of age and declined thereafter as a result of partial spontaneous separation (posterior vitreous detachment). This is plausible because no reference was made to posterior vitreous detachment status in the examined eyes, which would confound any attempts to correlate increasing thickness with increasing age, and also in the same study the intriguing observation of substantial (6-fold) variation in internal limiting membrane thickness between eyes from the same elderly patient.

Snead et al[45] immunohistochemically examined surgical specimens from 4 clinically distinct vitreomaculopathy subgroups; internal limiting membrane samples from patients in these subgroups (who had undergone no previous intraocular surgery or retinopexy) were compared with those of postmortem eyes (with and without uncomplicated posterior vitreous detachment). Basement membrane from the surgical internal limiting membrane specimens was the principal component identified in all 4 subgroups, with prominent hyperconvolution and reduplication of the internal limiting membrane apparent in the macular pucker and cellophane maculopathy subgroups. Although not discussed in this study, control light micrographs of postmortem eyes with uncomplicated senile posterior vitreous detachment seemed to show similar but less extensive duplication, thickening, contracture, and even schisis of the posterior hyaloid membrane. This is perhaps not surprising because systemic reduplication or lamellation of basement membranes frequently is found around capillaries in patients with diabetic microangiopathy,[46,47] and increasing basement membrane production is a well-characterized cellular response to aging and sublethal injury.[48]

Electron microscopy investigations of the posterior hyaloid membrane from donors with antemortem clinical confirmation of posterior vitreous detachment demonstrated a separately distinct membranous structure encasing the detached vitreous.[30] Low-magnification scanning electron micrography of the posterior aspect of a detached Weiss ring noted the irregular coarse appearance of the retinal aspect of the posterior hyaloid membrane and a smooth vitreal aspect adjacent to areas of fibrillar cortical gel, comparable with the cross-sectional and 3-dimensional reconstructions reported in the current study. High-magnification transmission electron micrographs depicted cross sections through extensively convoluted posterior hyaloid membranes with collagen fibrils inserting onto the vitreal aspect, in addition to scattered hemidesmosome attachment plaques.

Existing anatomic, molecular, and ultrastructural knowledge of the internal limiting membrane and its documented age-related changes, in addition to the limited investigations of the posterior hyaloid membrane, lend support to the findings we report herein. This demonstrates that the posterior hyaloid membrane is not simply a condensation of posterior vitreous cortex commonly referred to as the *posterior hyaloid face*, but rather a separately distinct true basement membrane structure that encases the extracellular matrix of the vitreous body. This basal lamina must originate from the surface of the retina during the process of posterior vitreous detachment and forms as a result of an anterior dehiscence of the retinal internal limiting membrane, which is known to peak in thickness in the age group when posterior vitreous detachment is most prevalent.

References

1. Kierszenbaum A, Tres L. *Histology and Cell Biology. An Introduction to Pathology*. 3rd ed. Philadelphia, PA: Elsevier; 2012.
2. Kleppel MM, Michael AF. Expression of novel basement membrane components in the developing human kidney and eye. *Am J Anat*. 1990;187:165-174.
3. Foos RY, Wheeler NC. Vitreoretinal juncture: synchysis senilis and posterior vitreous detachment. *Ophthalmology*. 1982;89:1502-1512.
4. Sebag J. Age-related changes in human vitreous structure. *Graefes Arch Clin Exp Ophthalmol*. 1987;225:89-93.
5. Benz MS, Packo KH, Gonzalez V, et al. A placebo-controlled trial of microplasmin intravitreous injection to facilitate posterior vitreous detachment before vitrectomy. *Ophthalmology*. 2010;117:791-797.
6. Ponsioen TL, Hooymans JM, Los LI. Remodelling of the human vitreous and vitreoretinal interface—a dynamic process. *Prog Retin Eye Res*. 2010;29:580-595.
7. Bishop PN. Structural macromolecules and supramolecular organisation of the vitreous gel. *Prog Retin Eye Res*. 2000;19:323-344.
8. Le Goff MM, Bishop PN. Adult vitreous structure and postnatal changes. *Eye (Lond)*. 2008;22:1214-1222.
9. Sebag J. Age-related differences in the human vitreoretinal interface. *Arch Ophthalmol*. 1991;109:966-971.
10. Sebag J. Anomalous posterior vitreous detachment: a unifying concept in vitreoretinal disease. *Graefes Arch Clin Exp Ophthalmol*. 2004;242:690-698.
11. Murakami K, Jalkh AE, Avila MP, et al. Vitreous floaters. *Ophthalmology*. 1983;90:1271-1276.

12. Snead MP, Snead DRJ, James S, Richards AJ. Clinicopathological changes at the vitreoretinal junction: posterior vitreous detachment. *Eye (Lond)*. 2008;22:1257-1262.
13. Akiba J. Prevalence of posterior vitreous detachment in high myopia. *Ophthalmology*. 1993;100:1384-1388.
14. Snead MP, Snead DR, Mahmood AS, Scott JD. Vitreous detachment and the posterior hyaloid membrane: a clinicopathological study. *Eye (Lond)*. 1994;8(Pt 2):204-209.
15. Weber-Krause B, Eckardt C. [Incidence of posterior vitreous detachment in the elderly]. *Ophthalmol Z Dtsch Ophthalmol Ges*. 1997;94:619-623.
16. Kičová N, Bertelmann T, Irle S, et al. Evaluation of a posterior vitreous detachment: a comparison of biomicroscopy, B-scan ultrasonography and optical coherence tomography to surgical findings with chromodissection. *Acta Ophthalmol*. 2012;90(4):e264-e268.
17. Kim YC, Harasawa M, Siringo FS, Quiroz-Mercado H. Assessment of posterior vitreous detachment on enhanced high density line optical coherence tomography. *Int J Ophthalmol*. 2017;10(1):165-167.
18. Mojana F, Kozak I, Oster SF, et al. Observations by spectral-domain optical coherence tomography combined with simultaneous scanning laser ophthalmoscopy: imaging of the vitreous. *Am J Ophthalmol*. 2010;149(4):641-650.
19. Bertelmann T, Goos C, Sekundo W, et al. Is optical coherence tomography a useful tool to objectively detect actual posterior vitreous adhesion status? *Case Rep Ophthalmol Med*. 2016;2016:3953147.
20. Johnson MW. Posterior vitreous detachment: evolution and role in macular disease. *Retina*. 2012;32(Suppl 2):S174-S178.
21. Kuhn F, Aylward B. Rhegmatogenous retinal detachment: a reappraisal of its pathophysiology and treatment. *Ophthalmic Res*. 2014;51:15-31.
22. Sebag J. *The vitreous: structure, function, and pathobiology*. New York: Springer-Verlag; 1989.
23. Stalmans P, Benz MS, Gandorfer A, et al. Enzymatic vitreolysis with ocriplasmin for vitreomacular traction and macular holes. *N Engl J Med*. 2012;367:606-615.
24. Steel DHW, Lotery AJ. Idiopathic vitreomacular traction and macular hole: a comprehensive review of pathophysiology, diagnosis, and treatment. *Eye (Lond)*. 2013;27(Suppl 1):S1-S21.
25. American Academy of Ophthalmology Retina Panel. Preferred Practice Pattern Guidelines: Posterior Vitreous Detachment, Retinal Breaks and Lattice Degeneration. San Francisco, CA: American Academy of Ophthalmology; 2008.
26. Dayan MR, Jayamanne DG, Andrews RM, Griffiths PG. Flashes and floaters as predictors of vitreoretinal pathology: is follow-up necessary for posterior vitreous detachment? *Eye*. 1996;10:456-458.
27. Byer NE. Natural history of posterior vitreous detachment with early management as the premier line of defense against retinal detachment. *Ophthalmology*. 1994;101:1503-1514.
28. Ang A, Poulson AV, Snead DR, Snead MP. Posterior vitreous detachment: current concepts and management. *Compr Ophthalmol Update*. 2005;6:167-175.
29. Kakehashi A, Takezawa M, Akiba J. Classification of posterior vitreous detachment. *Clin Ophthalmol Auckl N Z*. 2014;8:1-10.
30. Snead MP, Snead DRJ, Richards AJ, et al. Clinical, histological and ultrastructural studies of the posterior hyaloid membrane. *Eye (Lond)*. 2002;16:447-453.
31. Foos RY. Posterior vitreous detachment. *Trans Am Acad Ophthalmol Otolaryngol*. 1972;76:480-497.
32. Kohno T, Sorgente N, Ishibashi T, et al. Immunofluorescent studies of fibronectin and laminin in the human eye. *Invest Ophthalmol Vis Sci*. 1987;28:506-514.
33. Rhodes RH. An ultrastructural study of the complex carbohydrates of the mouse posterior vitreoretinal juncture. *Invest Ophthalmol Vis Sci*. 1982;22:460-477.
34. Fine BS. Limiting membranes of the sensory retina and pigment epithelium. An electron microscopic study. *Arch Ophthalmol*. 1961;66:847-860.
35. Fine BS, Tousimis AJ. The structure of the vitreous body and the suspensory ligaments of the lens. *Arch Ophthalmol*. 1961;65:95-110.
36. Daicker B, Guggenheim R, Gywat L. [Findings on retinal surface by scanning electron microscopy. II. Vitreous detachment]. *Graefes Arch Clin Exp Ophthalmol*. 1977;204:19-29.
37. Gärtner J. [The fine structure of the vitreous body cortex of the human eye at the ora serrata retinae in old age]. *Graefes Arch Clin Exp Ophthalmol*. 1965;168:529-562.
38. Hogan MJ, Alvarado JA, Weddell JE. *Histology of the Human Eye*. Philadelphia: Saunders; 1971.
39. Malecaze F, Caratero C, Caratero A, et al. Some ultrastructural aspects of the vitreoretinal juncture. *Int J Ophthalmol Z Für Augenheilkd*. 1985;191:22-28.
40. Masutani-Noda T, Yamada E. The mosaic pattern of the inner surface of vertebrate retina. *Arch Histol Jpn Nihon Soshikigaku Kiroku*. 1983;46:393-400.
41. Foos RY. Vitreoretinal juncture: topographical variations. *Invest Ophthalmol*. 1972;11:801-808.
42. Murphy C, Alvarado J, Juster R. Prenatal and postnatal growth of the human Descemet's membrane. *Invest Ophthalmol Vis Sci*. 1984;25:1402-1415.
43. Danysh BP, Duncan MK. The lens capsule. *Exp Eye Res*. 2009;88:151-164.
44. Heegaard S. Structure of the human vitreoretinal border region. *Int J Ophthalmol Z Für Augenheilkd*. 1994;208:82-91.
45. Snead DRJ, Cullen N, James S, et al. Hyperconvolution of the inner limiting membrane in vitreomaculopathies. *Graefes Arch Clin Exp Ophthalmol*. 2004;242:853-862.
46. Fischer VW, Barner HB, LaRose LS. Quadriceps and myocardial capillary basal laminae. Their comparison in diabetic patients. *Arch Pathol Lab Med*. 1982;106:336-341.
47. Vracko R. Basal lamina layering in diabetes mellitus. Evidence for accelerated rate of cell death and cell regeneration. *Diabetes*. 1974;23:94-104.
48. Martinez-Hernandez A, Amenta PS. The basement membrane in pathology. *Lab Investig J Tech Methods Pathol*. 1983;48:656-677.

Footnotes and Financial Disclosures

Originally received: April 26, 2017.
Final revision: July 11, 2017.
Accepted: August 1, 2017.
Available online: September 1, 2017. Manuscript no. 2017-970.

[1] Vitreoretinal Service, Addenbrooke's Hospital, Cambridge University Hospitals NHS Foundation Trust, Cambridge, United Kingdom.

[2] Department of Histopathology, Coventry Hospital, University Hospitals Coventry and Warwickshire NHS Trust, Coventry, United Kingdom.

[3] Department of Pathology, University of Cambridge, Cambridge, United Kingdom.

[4] Research Department of Cell and Developmental Biology, University College London, London, United Kingdom.

[5] Regional Molecular Genetic Laboratory, Addenbrooke's Hospital, Cambridge University Hospitals NHS Foundation Trust, Cambridge, United Kingdom.

[6] Institute of Ophthalmology, University College London, London, United Kingdom.

Presented at: The 45th Cambridge Symposium, September 2015, Cambridge, United Kingdom; and the Oxford Ophthalmological Congress, July 2015, Oxford, United Kingdom.

Financial Disclosure(s):

Supported by University of Cambridge Retinal Research Fund, Cambridge, United Kingdom; and the Annie Arnold Research Legacy Fund. The sponsor or funding organization had no role in the design or conduct of this research.

HUMAN SUBJECTS: Ocular tissue included in this study was obtained from donated human eyes following corneal harvesting for transplantation. This project was conducted after National Research Ethics Service approval (identifier 05/Q2802/77), and all investigations were conducted in accordance with the tenets of the Declaration of Helsinki with regard to research on human tissue.

Author Contributions:

Conception and design: Fincham, Poulson, McNinch, D.Snead, Limb, M.P.Snead

Analysis and interpretation: Fincham, James, Spickett, Hollingshead, Thrasivoulou, Richards, D.Snead, Limb, M.P.Snead

Data collection: Fincham, James, Spickett, Hollingshead, Thrasivoulou, Richards

Obtained funding: none

Overall responsibility: Fincham, M.P.Snead

Abbreviations and Acronyms:
PVD = posterior vitreous detachment.

Correspondence:
Martin P. Snead, MD, FRCOphth, Vitreoretinal Research Group, Vitreoretinal Service, Box 41, Addenbrooke's Hospital, Hills Road, Cambridge University Hospitals NHS Foundation Trust, Cambridge, Cambridgeshire CB2 2QQ, United Kingdom. E-mail: mps34@cam.ac.uk.

Pictures & Perspectives

Imaging of Neovascular Membrane Over a Choroidal Osteoma by OCT Angiography

A 26-year-old man presented with a 5-month history of blurry vision, photopsia, and metamorphopsia of the right eye. Retinal examination showed a geographic orange-yellow calcified macular lesion, with retinal pigment epithelium (RPE) mottling and subtle hemorrhage (Fig 1**A**), suggesting a choroidal neovascular membrane (CNVM). An OCT angiography (OCTA) showed an increased capillary density (Fig 1**B** and **C**, *white arrows*), identifying a juxtafoveal CNVM along the edge of the tumor, at the level of the choroid capillary plexus (Fig 1**B**) and the external plexiform layer (Fig 1**C**). Although CNVM diagnosis may be hindered by inherent hyperfluorescence seen on fluoroangiography, OCTA might accurately and noninvasively detect CNVM. (Magnified version of Fig 1A-C is available online at www.aaojournal.org.)

Ana Beatriz D. Grisolia, MD
Maira de França Martins, MD
Hakan Demirci, MD

Department of Ophthalmology and Visual Sciences, Kellogg Eye Center, University of Michigan Medical School, Ann Arbor, Michigan